Prediction of Nonlinear Distortion in HTS Filters for CDMA Communication Systems

C. Collado, J. Mateu, R. Ferrús, and J. M. O'Callaghan

***Abstract*—HTS materials are known to produce intermodulation and other nonlinear effects, and this may restrict their use in wireless communication systems. While significant efforts are being done to measure and characterize nonlinear properties of HTS materials, there are very few works that relate these properties to system parameters. In this work we attempt to bridge this gap by using Harmonic Balance algorithms to analyze the nonlinear performance of superconducting filters subject to the WCDMA signals specified by 3GPP for the UMTS wireless system. This is a first step to predict compliance with system parameters like Adjacent Channel Leakage power Ratio (ACLR) or Error Vector Magnitude (EVM).**

***Index Terms*—CDMA, harmonic balance, HTS, intermodulation, nonlinearities, superconducting filters.**

I. Introduction

THIRD-GENERATION (3G) wireless systems are designed for multimedia applications, where high data rates will be available for person-to-person communication and/or access to information and services on public and private networks. These systems are based on spread spectrum techniques where CDMA signals are used to multiplex users onto the same frequency channel using Orthogonal Variable Spreading Factor (OVSF) and Gold-code scrambling. To maintain high spectral efficiency in dense electromagnetic environments, filtering is essential to separate the desired frequency band from other signals. Passband filters with High Temperature Superconductors (HTS) might be very well suited for this application, but they are known to exhibit nonlinear effects giving rise to intermodulation distortion, even at moderate power levels. These nonlinear effects in HTS filters are distributed along the structure of the device and can degrade the performance of the whole transceiver [1], [2].

In previous works we have proposed numerical techniques based on Harmonic Balance (HB) to predict microwave nonlinear response of HTS filters and resonators when one or two sinusoidal signals are applied to them [3]. This is not sufficient to quantify the performance of a 3G communication system, which is subject to much more complex CDMA signals and whose nonlinearities might affect important system parameters such as adjacent channel leakage power ratio (ACLR) or error vector magnitude (EVM).

In this work we have extended the flexibility of our numerical methods based on HB to simulate HTS filters subject to signals with many frequency components like those of CDMA systems. We refer to this method as Multitone Multiport Harmonic Balance (MMHB). We present illustrative examples which show the viability of this kind of analysis for HTS front-end receivers and transmitters in 3G systems.

Manuscript received August 6, 2002. This work is supported by the Spanish Ministry of Science and Technology under Project TIC2000-0996 and Scholarship AP99-78085980 for J. Mateu, and by Generalitat de Catalunya (DURSI) under Grant 2001 SGR 0026.

C. Collado, R. Ferrús, and J. M. O'Callaghan are with Universitat Politècnica de Catalunya (UPC), Campus Nord UPC D3 08034 Barcelona, Spain (e-mail: joano@tsc.upc.es).

J. Mateu is with CTTC-Centre Tecnològic de Telecomunicacions de Catalunya, Edifci NEXUS, 08034 Barcelona, Spain.

Digital Object Identifier 10.1109/TASC.2003.813723

II. Multitone Multiport Harmonic Balance

Our simulations model the distributed nonlinearities in HTS filters by discretizing its structure (for example breaking down transmission lines in segments much shorter than a wavelength). A large nonlinear equivalent circuit results (see, for example, Figs. 1 and 2 in [4]), and is analyzed using numerical methods based on HB [5]. Common to all HB algorithms is the splitting between the linear part of the circuit, characterized in frequency-domain, and the nonlinear one, characterized in time-domain. For example, in a transmission line filter, the nonlinear part of the circuit would model the nonlinearities in the resistance and inductance per unit length of the transmission line, and the linear network would model all other (linear) elements in the circuit (the linear resistance, inductance, capacitance and conductance per unit length of the line, the coupling between lines, etc.) [4].

The linear part is a $(N+1)$-port with N of its ports loaded with nonlinear elements and the remaining one is fed by the source(s) driving the circuit. This $(N+1)$-port is characterized by its impedance matrix ($\mathbf{Z}$) which relates the voltage dropped across the N ports (V_L) to the current flowing out of the network (I_L) and impressed on the N nonlinear elements. In principle, the values of the matrix elements have to be calculated at all frequencies of the source current, and at all other frequencies where spurious signals may exist. The nonlinear part consists of N nonlinear one-port elements modeling a distributed nonlinearity. In this work we will focus on nonlinearities where the voltage v_{NL} across each one-port depends on the current though it (i_{NL}) by means of a nonlinear resistance ($\Delta R(i_{NL})$) and inductance ($\Delta L(i_{NL})$), i.e.,:

$$v_{NL}(i_{NL}) = \Delta R(i_{NL}) i_{NL} + \frac{d}{dt}\left[\Delta L(i_{NL}) i_{NL}\right] \quad (1)$$

which is used to model HTS filters with transmission line [4] or disk resonators [6]. As shown in [3], this can be extended to cavities with HTS endplates, or to planar filters whose resonators have convoluted layouts.

As detailed in [5], HB is based on an iterative procedure which matches the voltage and current variables of the linear

(V_L and I_L) and nonlinear part (V_{NL} and I_{NL}). Transformation algorithms are needed to convert the data from frequency to time domain and vice versa, so that the linear part can be solved in frequency domain and the nonlinear part in time domain. A review of such algorithms is given in [7].

A key difference of MMHB algorithm with respect to other numerical methods that we have previously used to simulate HTS devices is the need for sampling the voltages and currents in the device equivalent circuit. Unlike in a two-tone intermodulation experiment, the HTS device is now fed with a broadband signal with a carrier frequency f_0 and bandwidth B, and square law nonlinearities in the device produce voltages and currents whose spectral components will be distributed across two frequency bands of bandwidth $3B$ centered at f_0 and $3f_0$. Undersampling is necessary to take into account all these frequency components and down convert the signal to baseband. The sampling rate has to be carefully chosen to avoid aliasing. Details on these aspects will be given in a forthcoming paper.

The preceding discussions result in the following outline of the MMHB method:

1) Once the frequency resolution Δf is decided, we calculate the frequencies of the spectral lines to be considered.
2) Calculation of the matrix $\mathbf{Z}$ in a $3B$ bandwidth centered at f_0 in steps of Δf.
3) Determination of the sampling rate f_s and the frequencies of the down-converted signals.
4) Start the Harmonic Balance iterative algorithm (see [3, Fig. 3]):
    a) Propose a solution for the time-domain current across the N nonlinear one-ports (i_{NL}). The initial estimate is calculated with the matrix $\mathbf{Z}$, assuming that the voltage across these one-ports is zero.
    b) With the down-converted version of i_{NL}, find the voltage across the nonlinear one-ports v_{NL} by applying an equivalent of (1) that takes into account the effects of taking a time derivative to a down-converted signal.
    c) Transform v_{NL} to frequency domain and find its up-converted counterpart.
    d) With the voltage resulting from the previous point, the source current I_s, and the matrix $\mathbf{Z}$, solve the linear circuit and find an updated estimate of the current thought the one-ports I_{NL}.
    e) Down-convert I_{NL} and transform it to time domain. Compare it with i_{NL} in point (b) above. If convergence is not achieved go to point (b) and start a new iteration.

III. Examples

In this section we illustrate the usefulness of MMHB by calculating some figures of merit (Spurious Free Dynamic Range (SFDR), ACLR and EVM) which can be affected by the nonlinearities in HTS filters. We have analyzed a number of passband filters at UMTS frequencies with Chebyshev and quasielliptic designs having various types of resonators, bandwidth and order. All the filters have been designed for a return loss of 20 dB. The quasielliptic designs had a single pair of transmission zeros, with a ratio of the bandwidth between zeros to the 3 dB bandwidth of 1.2 [8]. Three resonator types have been considered: microstrip half-wave resonant lines with either a 50 or 25 Ω characteristic impedance, and TM_{010} disk resonators. Two different bandwidths were considered: 5 and 15 MHz, to allow for a passband with either one or three UMTS channels.

In all cases we have assumed a 0.5 mm thick MgO substrate with a 700 nm thick Y-Ba_2-Cu_3-$O_{7-\delta}$ film whose nonlinearities are due to a dependence of the penetration depth λ with current density j of the type:

$$\lambda(j) = \lambda(0)\left(1 + \frac{0.5|j|}{j_{IMD}}\right) \tag{2}$$

with $j_{IMD} = 5 \times 10^{12}$ Am^{-2}[9]. With this dependence, we have determined the variation with respect to the small-signal values of the resistance per unit length ($\Delta R(i)$) and inductance per unit length ($\Delta L(i)$) of the halfwave transmission line resonators, so that $\Delta L(i)$ and $\Delta R(i)$ can be used in (1) to find the voltage along the line v_{NL} due to the nonlinearities of the HTS. The calculation of $\Delta L(i)$, $\Delta R(i)$ from (2) is done following the procedure in described in [10]. For 50 Ω lines we have obtained $\Delta R(i) = 1.68 \times 10^{-3}|i|$ Ωm^{-1} and $\Delta L(i) = 2.66 \times 10^{-12}|i|$ Hm^{-1}. For 25 Ω lines the result is $\Delta R(i) = 2.1 \times 10^{-4}|i|$ Ωm^{-1} and $\Delta L(i) = 3.29 \times 10^{-13}|i|$ Hm^{-1}.

For the TM_{010} disk resonators, the effect of the nonlinearities is to create a radial electric field e_{NL} that will have a nonlinear dependence with surface current density [6], [9], [11]. If the nonlinearities are predominantly reactive [11]$e_{NL} \approx d/dt\,(b_{NL}(j_s)j_s)$ which, combined with (2) and the value of j_{IMD} above results in $b_{NL}(j_s) = 1.25 \times 10^{-19}|j_s|$H [9]. As detailed in [6] this can be transformed in a nonlinear inductance $\Delta L = 2b_{NL}/2\pi\rho$ (where ρ is the radial position of the discretization cell being considered) that can be used in an equivalent of (1).

A. Two Tone Nonlinear Response: SFDR

The Spurious Free Dynamic Range (SFDR) of a device is the ratio between the noise floor and the power of the sinusoidal signals that, when applied to the device in a two-tone intermodulation measurement, generate intermodulation products whose power is equal to the noise floor [12]. In this work, we have used a noise floor of -108 dBm [13]. Since the signals applied to the device to quantify its SFDR are sinusoidal, we can either use our previous versions of HB for HTS analysis (which are restricted to sinusoidal signals) [3], or the MMHB described here (which can handle a wide variety of signals, among them sinusoidal ones). The SFDR examples shown below have been calculated with both codes, to confirm the proper operation of the MMHB described here, and we found that the results of both codes agreed.

As an example of the type of results obtained, Fig. 1 shows the SFDR obtained for the third order intermodulation product by sweeping two tones across the band pass of three different filters and keeping a constant spacing (62.5 KHz) between them. The filters simulated had 50 Ω lines and were designed for a 15 MHz bandwidth. Two of them had a Chebyshev designs of orders 8 and 12, and the third one had an 8th order quasielliptic design. The figure shows that for 8th order filters, the SFDR of

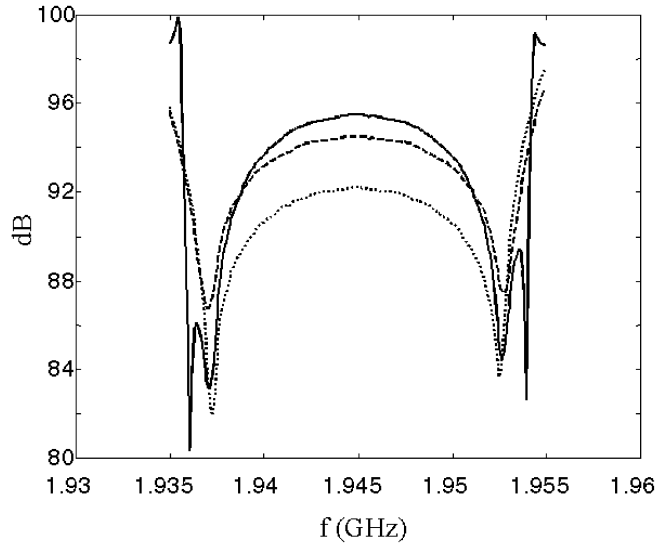

Fig. 1. Spurious-free dynamic range for three different filters with identical 15-MHz bandwidth and 50-Ω line resonators. Continuous line: eighth order quasieliptic filter. Dashed line: eighth order Chebyshev filter. Dotted line: twelfth order Chebyshev filter.

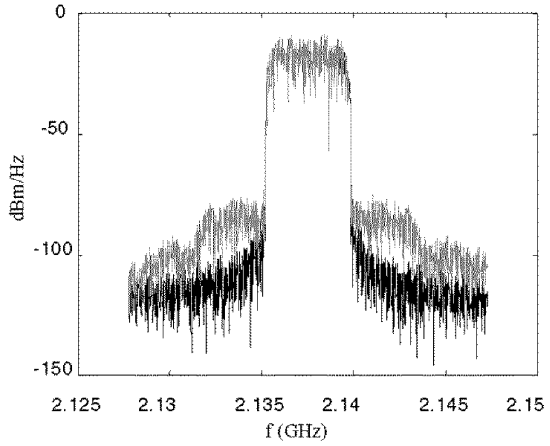

Fig. 2. WCDMA spectrum before (black) and after (grey) an HTS filter ($QE\_D\_O_8BW_{15}$) as simulated by MMHB, showing the effect of the nonlinearities in the regrowth of the spectrum outside the passband. The input signal is a sequence of 77 bits (one user with a spreading factor $SF = 8$) with QPSK modulation and complex spreading. Carrier frequency is 2.1375 GHz and power $P_0 = 43$ dBm. The resulting ACLR of the signal at the filter output is 68.8 dB. Note that this is only an illustrative example: more users would give lower ACLR.

the quasielliptic filter is slightly better than that of the Chebyshev filter at the center of the bandwidth, but can be 6 dB smaller if the two input tones are at the edge of the pass band. On the other hand, increasing the order in the Chebyshev filter from 8 to 12 causes a degradation between 3 and 5 dB of the SFDR. This example shows that for Chebyshev filters, increasing the order of the filter reduces the SFDR. Other simulations have shown that this has also happens in quasielliptic filters.

An extensive study has been made to compare the SFDR of various coupled-line filters of identical order. The study has shown that the SFDR of various 12th order filters at the center of the passband changes little (less than 1 dB) with the type of filter (Chebyshev or quasielliptic). Filters with 5 MHz bandwidth and 50 Ω lines have the smallest SFDR (88 dB), which increases to 90 dB if the impedance of the lines is decreased to 25 Ω. An SFDR of 93 dB is obtained for 15 MHz filters with 50 Ω lines, which can be increased to 97 dB by using 25 Ω lines.

B. Multitone Nonlinear Response: ACLR and EVM

As pointed out in [14], the SFDR and the third order intercept point are not sufficient to quantify the performance degradation caused by a nonlinear device when it is subject to spread spectrum signals as those in a 3G communication systems. To characterize such degradation, other parameters such as ACLR and EVM are used.

ACLR is a figure of merit that quantifies the leakage of the transmitted power into adjacent channels, and therefore accounts for the combined effects of filter selectivity and spectral regrowth due to nonlinear effects. Fig. 2 shows how these effects increase the spectral components of the signal outside the passband. Qualitatively similar results have been obtained from measurement of HTS filters [15]. With this spectrum, and following a procedure specified in [16], we can calculate the ACLR of the signal.

EVM quantifies the modulation accuracy by making a bit by bit comparison between the distorted waveform and the original one. It therefore accounts, among others, for the in-channel effects of the nonlinearities. To calculate EVM from our simulated data, we have used [17]:

$$EVM = \sqrt{\text{mean}\left[\left|\frac{V_d}{V_{d,RMS}}e^{-j\Delta\phi} - \frac{V_i}{V_{i,RMS}}\right|^2\right]} \qquad (3)$$

being V_d the distorted signal, V_i the ideal signal without nonlinear distortion, $V_{d,RMS}$ and $V_{i,RMS}$ their respective RMS values and $\Delta\phi$ the mean value of the phase difference between distorted and ideal signals. Equation (3) accounts for the mean of the phase deviation $\Delta\phi$, therefore it is appropriate if the receiver is able to correct this. Otherwise, the EVM would be greater and it should be calculated with $\Delta\phi = 0$ (we use EVM_0 in that case).

In order to quantify the degradation of the EVM caused only by the nonlinearities of the filter we have defined the ratio between the EVM obtained from nonlinear simulations to that obtained if the filter was a linear device.

$$R = \frac{EVM}{EVM_{lin}} \qquad (4)$$

Table I shows the SFDR (at midband), ACLR, EVM and R for a set of filters whose input signal is made up of a sequence of 77 bits (one user with a spreading factor $SF = 4$) with QPSK modulation and complex spreading. Carrier frequency is 2.1375 GHz and power $P_0 = 43$ dBm. Even though longer bit streams would be desirable for a more reliable quantitative characterization of these parameters, some qualitative statements about how these filters compare can be made. The first is the expected effect on bandwidth: all parameters degrade at smaller bandwidths due to the higher circulating power in the filter. This is very clear by looking at the last column in the table where the values of R show that the EVM due to the filter nonlinearities

TABLE I
COMPARISON AMONG VARIOUS TYPES OF FILTERS

TYPE	Order	BW	SFDR	ACLR	EVM	EVM_0	R
CH	**6**	**15**	106.0	70.6	0.2	0.4	1.1
QE	**6**	**15**	107.6	73.2	0.2	0.3	1.0
CH	**8**	**15**	104.2	67.2	0.2	0.5	1.1
QE	**8**	**15**	105.1	68.8	0.2	0.4	1.1
CH	**6**	**5**	98.8	59.2	0.4	2.0	2.2
QE	**6**	**5**	100.4	62.1	0.4	1.5	2.3
CH	**8**	**5**	97.0	57.3	0.5	3.1	2.9
QE	**8**	**5**	98.0	59.3	0.6	2.7	3.7

[1] CH stands for Chebyshev design and QE for Quasi-Elliptic design.
[2] BW in MHz. All other parameters are dimensionless.

is much higher in the filters with 5 MHz bandwidth. Similarly, higher filter orders result in steeper slopes in the transfer function at the passband edge, and this is known to be detrimental for intermodulation performance. As a result, all parameters in Table I degrade when the order is increased. In other words, increasing the filter order improves its selectivity and its ability to reject out of band interfering signals, but has a detrimental effect in the in-band nonlinear effects. Finally, quasielliptic filters are slightly better than Chebyshev ones (of identical order and bandwidth) in SFDR and ACLR. Their EVM are very similar, but their EVM_0 indicates that Chebyshev filters produce more phase deviation ($\Delta\phi$) due to nonlinearities.

IV. CONCLUSIONS

We have described the basics of the extension of our Harmonic Balance algorithms to allow them to analyze the effects of signals with many frequency components on High Temperature Superconductors. This capability is of interest since it allows to evaluate the effect of superconductor nonlinearities in filters subject to CDMA signals. The extended algorithm (MMHB) compares well with the previous ones when analyzing two-tone intermodulation, and is producing reasonable results when predicting the performance of HTS filters with 3G CDMA signals.

REFERENCES

[1] B. Willemsen, "HTS wireless applications," in *Microwave Superconductivity*, H. Weinstock and M. Nisenoff, Eds: NATO Science Series, 2001, vol. 375, pp. 387–387.

[2] B. A. Willemsen, "HTS filter subsystems for wireless telecomunications," *IEEE Trans. Appl. Supercond.*, vol. 11, no. 1, pp. 60–67, 2001.

[3] C. Collado, J. Mateu, J. Parron, J. Pons, J. M. O'Callaghan, and J. M. Rius, "Harmonic balance algorithms for the nonlinear simulation of HTS devices," *J. Supercond.*, vol. 14, no. 1, pp. 57–64, 2001.

[4] C. Collado, J. Mateu, and J. M. O'Callaghan, "Nonlinear simulation and characterization of devices with HTS transmission lines using harmonic balance algorithms," *IEEE Trans. Appl. Supercond.*, vol. 11, no. 1, pp. 1396–1399, 2001.

[5] S. A. Maas, *Nonlinear Microwave Circuits Publisher*: Artech House, 1988.

[6] J. Mateu, C. Collado, and J. M. O'Callaghan, "Nonlinear analysis of disk resonators. Application to material characterization and filter design," *IEEE Trans. Appl. Supercond.*, vol. 11, no. 1, pp. 135–138, 2001.

[7] V. Borich, J. East, and G. Haddad, "An efficient fourier transform for multitone harmonic balance," *IEEE Trans. Microwave Theory Tech.*, vol. 47, no. 2, p. 182, 1999.

[8] J.-S. Hong and M. J. Lancaster, "Design of highly selective microstrip bandpass filters with a single pair of attenuation poles at finite frequencies," *IEEE Trans. Microwave Theory Techn.*, vol. 48, no. 7, pp. 1098–1107, 2000.

[9] C. Collado, J. Mateu, T. J. Shaw, and J. O'Callaghan, "HTS nonlinearities in microwave disk resonators," Physica C, to be published.

[10] T. Dahm and D. J. Scalapino, "Theory of intermodulation in superconducting microstrip resonator," *J. Appl. Phys.*, vol. 81, no. 4, p. 2002, 1997.

[11] T. Dahm, D. J. Scalapino, and B. A. Willemsen, "Microwave intermodulation of a superconducting disk resonator," *J. Appl. Phys.*, vol. 86, no. 7, p. 1, 1999.

[12] D. M. Pozar, *Microwave and RF Design of Wireless Systems.* New York: Wiley, 2001, pp. 348–349.

[13] H. Holma and A. Toskala, *WCDMA for UMTS Radio Access for Third Generation Mobile Communication*. New York: Wiley, 2000, p. 182.

[14] K. G. Gard, H. M. Gutierrez, and M. B. Steer, "Characterization of spectral regrowth in microwave amplifiers based on the nonlinear transformation of complex gaussian process," *IEEE Trans. Microwave Theory Tech.*, vol. 47, no. 7, pp. 1059–1069, 1995.

[15] A. P. Jenkins, D. Dew-Hughes, and D. J. Edwards, "Application of TBCCO based HTS devices to digital cellular communications," *IEEE Trans. Appl. Supercond.*, vol. 9, no. 2, pp. 2849–2852, 1999.

[16] "BS Radio Transmission and Reception (FDD)," 3GPP TS 25.104 V5.2.0 (2002–2003).

[17] *Design Methodology and Implementation of a 3rd Generation W-CDMA Transceiver using Deep Submicron CMOS Technologies*, Project acronym: LEMON, 2000, p. 62.